Research Article

Experimental Evaluation of the Density Ratio Effects on the Cooling Performance of a Combined Slot/Effusion Combustor Cooling System

Antonio Andreini, Gianluca Caciolli, Bruno Facchini, and Lorenzo Tarchi

DIEF, Department of Industrial Engineering Florence, University of Florence, Via S. Marta 3, 50139 Florence, Italy

Correspondence should be addressed to Bruno Facchini; bruno.facchini@htc.de.unifi.it

The purpose of this study is to investigate the effects of coolant-to-mainstream density ratio on a real engine cooling scheme of a combustor liner composed of a slot injection and an effusion array with a central dilution hole. Measurements of heat transfer coefficient and adiabatic effectiveness were performed by means of steady-state thermochromic liquid crystals technique; experimental results were used to estimate, through a 1D thermal procedure, the Net Heat Flux Reduction and the overall effectiveness in realistic engine working conditions. To reproduce a representative value of combustor coolant-to-mainstream density ratio, tests were carried out feeding the cooling system with carbon dioxide, while air was used in the main channel; to highlight the effects of density ratio, tests were replicated using air both as coolant and as mainstream and results were compared. Experiments were carried out imposing values of effusion blowing and velocity ratios within a range of typical modern engine working conditions. Results point out the influence of density ratio on film cooling performance, suggesting that velocity ratio is the driving parameter for the heat transfer phenomena; on the other hand, the adiabatic effectiveness is less sensitive to the cooling flow parameters, especially at the higher blowing/velocity ratios.

1. Introduction

In the course of last years, the increase of performances for the gas turbine for aeronautics has been achieved by increasing the pressure ratio and the maximum cycle temperature. These working conditions are not bearable with the materials employed in the components exposed to high thermal loads; hence, the development of effective cooling schemes is fundamental to match the increasing trend of gas turbine operating temperature. On the other hand, the development of aeroengine combustor is driven also by the effort to reduce NO_x emissions, in order to meet stricter legislation requirements.

To satisfy future ICAO standards concerning NO_x emissions, main engine manufacturers have been updating the design concept of combustors. Future aeroengines combustion devices will operate with very lean mixtures in the primary combustion zone, switching as much as possible to premixed flames. Whatever detailed design will be selected, the amount of air in the primary zone will grow significantly at the expense of liner cooling air, which thus will be reduced. Consequently, important attention must be paid to the appropriate design of the liner cooling system in order to optimize coolant consumption and guarantee an effective liner protection. In addition, further goals need to be taken into account: reaction quenching due to a sudden mixing with cooling air should be accurately avoided, whilst temperature distribution has to reach the desired levels in terms of OTDF.

In recent years, the improvement of drilling capability has allowed making a large quantity of extremely small cylindrical holes, whose application is commonly referred to as effusion cooling. Alternative solutions to the typical 2D-slot combustor cooling systems, like the full coverage film cooling or multihole film cooling, still relies on the generation of a high effective layer of film cooling; on the contrary, an

effusion cooling system permits to lower the wall temperature mainly through the so-called "heat sink effect," which is the wall cooling due to the heat removed by the passage of the coolant through the holes [1, 2]. A high number of small tilted holes homogeneously distributed over the whole surface of the liner allows, if accurately designed, a significant improvement in lowering wall temperature, despite a slight reduction of the wall protection at least in the first part of the liner. Even if early effusion cooling schemes were developed to be an approximation of transpiration cooling, the design of effusion cooling in current combustor is usually based on very shallow injection holes ($\alpha \leq 30°$) with high coolant jet momentum; this solution allows to greatly increase the heat sink effect (higher holes Reynolds number and higher exchange areas) without excessive detriment to film effectiveness. With this design approach, the analysis and the characterization of the heat transfer and the wall protection due to the injection of coolant become a fundamental issue in order to estimate the entire cooling system performance.

Many studies of full coverage film cooling have been focused on measuring or estimating the film effectiveness generated by coolant jets and the heat transfer of effusion cooling. Scrittore et al. [3] studied the effects of dilution hole injection on effusion behaviour; they found relevant turbulence levels downstream dilution holes, thus leading to an increased spreading of coolant jets. Scrittore et al. [4] measured velocity profiles and adiabatic effectiveness of a full coverage scheme with blowing ratios from 3.2 to 5.0, finding the attainment of a fully developed effectiveness region at the 15th row and a very low effect of blowing ratio on cooling performance. Metzger et al. [5] studied the variation of heat transfer coefficient for full-coverage film cooling scheme with normal holes, founding an augmentation of 20–25% in the local heat transfer with blowing ratio 0.1 and 0.2. Crawford et al. [6] experimentally determined Stanton number for an effusion cooling geometry. Martinez-Botas and Yuen [7] measured heat transfer coefficient and adiabatic effectiveness of a variety of geometries in a flat plate to test the influence of the injection angle by varying blowing ratio from 0.33 to 2.0. They measured the variation of the heat transfer coefficient h with respect to a reference case h_0; results show that there is a maximum of h/h_0 close to the hole and further downstream with highest heat transfer augmentation for 30° injection angle. Kelly and Bogard [8] investigated an array of 90 normal holes and found that the largest values for h/h_0 occur immediately downstream of the film cooling holes and the levels of h/h_0 are similar for the first 9 rows. They explained that this could be due to an increase in the local turbulence levels immediately downstream of the holes, created by the interaction between the cooling jet and the mainstream flow. Another reason could be the creation of a new thermal boundary layer immediately downstream of the cooling jets. In the open literature, none of the previous studies investigates the effect that a high blowing ratio has on adiabatic effectiveness, heat transfer coefficient, and Net Heat Flux Reduction. As reported by Kelly and Bogard [8], increases in heat transfer coefficient due to high blowing ratios could potentially be replaced by an increase in heat transfer coefficient due to high mainstream turbulence.

More recently Facchini et al. [9, 10] measured the overall effectiveness and the heat transfer coefficient at variable blowing ratios on a real engine cooling scheme to evaluate the combined effects of slot, effusion, and a large dilution hole; they found that an increase in BR leads to lower values of effectiveness. On the other hand, they found that high BR values enhance the heat transfer phenomena. Facchini et al. [11] investigated also the influence of a recirculating area in the mainstream on the same geometry; they highlight that the presence of the recirculation leads to a general reduction of effectiveness, while it does not have significant effects on the heat transfer coefficient.

Despite many studies deal with the investigation of the effusion cooling performance, most of them were conducted by using air as coolant and mainflow, precluding the possibility to point out the effects of density ratio between the two flows. Density ratio is, however, a key parameter for the design of a liner cooling system, mainly because of the actual large temperature difference between coolant and burned gases inside the core of the combustor. Ekkad et al. [12, 13] measured effectiveness and heat transfer coefficient distribution over a flat surface with one row of injection holes inclined streamwise at 35° for several blowing ratios and compound angles; tests were carried out by using air and carbon dioxide as coolant, finding that both heat transfer and effectiveness increase with blowing ratio. They also pointed out the effects of density ratio, showing how these effects are more evident with increasing the compound angle and the momentum flux ratio. This experimental survey was, however, oriented for turbine blade applications rather than combustors. More recently, Lin et al. [14, 15] investigated both experimentally and numerically adiabatic film cooling effectiveness of four different 30° inclined multihole film cooling configurations; the survey, which was specific for combustor liner applications, was performed by using a mixture of air and CO_2 as coolant, but it was mainly focused on studying the influence of hole geometrical parameters and blowing ratio on film cooling rather than on the effects of density ratio. Andreini et al. [16] performed a CFD analysis on the a test article which replicated a slot injection and an effusion array; they simulated the behaviour of the cooling system both with air and CO_2. Numerical results show that the entity of local heat transfer enhancement in the proximity of effusion holes exit is due to gas-jets interaction and that it mainly depends on effusion velocity ratio; furthermore, a comparison between results obtained with air and with CO_2 as coolant pointed out the effects of density ratio, showing the opportunity to scale the increase in heat transfer coefficient with effusion jets velocity ratio.

In the present study, the effects of density ratio on heat transfer coefficient, adiabatic effectiveness, NHFR, and overall effectiveness are investigated on a test rig which replicates a real cooling system for a combustor liner application, made up of a slot, an effusion array, and a dilution hole. In order to reproduce a representative value of combustor coolant-to-mainstream density ratio, tests were carried out by feeding the cooling system with carbon dioxide (CO_2), while air was used in the main channel; the test plate was tested imposing several values of blowing and velocity ratios within the range of

typical modern engine working conditions. To highlight the effects of density ratio and, as a consequence, to distinguish between the influence of blowing ratio and velocity ratio, tests were replicated by using air both as coolant and mainstream and results were compared. Results point out the influence of DR on the performance of the cooling scheme; moreover, they give useful indications on how to take into account the density ratio effects without using a foreign gas in a low temperature lab-scaled facility.

2. Experimental Facility

This investigation was aimed at pointing out the dependence of film cooling performance on coolant-to-mainstream density ratio. In order to achieve this goal, measurements on a test rig which represents a specific cooled combustor liner were carried out by using air and carbon dioxide (CO_2) as cooling flows and results were compared in terms of heat transfer coefficient (HTC), adiabatic effectiveness (η_{aw}), Neat Heat Flux Reduction (NHFR), and overall effectiveness (η_{ov}).

The test rig, depicted in Figure 1, consists of an open-loop suction type wind tunnel which allows the complete control of three separate flows: the hot mainstream, the slot cooling, and the effusion cooling flows. The vacuum system is made up of two rotary vane vacuum pumps with a capacity of 900 m^3/h each dedicated to the extraction of the mainstream mass flow.

The mainstream flow rate is set up by guiding the speed of the pumps and using a calibrated orifice located at the beginning of the wind tunnel (throttle). The mainstream temperature is set up by using a 24.0 kW electronically controlled electric heater, placed at the inlet of the rig.

Slot and effusion coolant flows reach the test rig crossing two different lines that connect the wind tunnel with a pressure tank which stores the cooling fluid up to a maximum pressure of 1 MPa. Flow rates are set up by throttling two separated valves. Heaters for a total power of 1.5 kW are placed along the lines which connect the tank to the rig in order to set the desired inlet coolant temperature.

The mass flow rate is measured at three different locations of the rig: according to the standard EN ISO 5167-1 one orifice measures the flow rate blown by the pumps, while two orifices measure the slot and the effusion mass flow rates.

Two pressure scanners Scanivalve DSA 3217 with temperature compensated piezoresistive relative pressure sensors measure the static pressure in 32 different locations with a maximum accuracy of 6.9 Pa. Several T type thermocouples connected to a data acquisition/switch unit (HP/Agilent 34970A) measure the mainstream and the coolant static temperatures.

The main channel has a constant cross-section of 100 × 150 mm and is 1000 mm long. In the first part of the channel the mainstream flow crosses a honeycomb and three screens which allow to set an uniform velocity profile. A 6.0 mm square hole grid (hole pitch 7.6 mm, plate thickness 0.7 mm) is placed 125 mm upstream the slot coolant injection, so as to set turbulence level at $x/S_x = 0$ around 5%, with a macroscopic length scale of 2.8 mm, according to correlations proposed by Roach [17].

Heat transfer coefficient and effectiveness are determined by a steady-state technique, measuring wall temperatures from a heated surface by means of TLC paint. Wide band TLC $30C20W$ supplied by Hallcrest and active from ~30°C to 50°C are used. Crystals are thinned with water and sprayed with an airbrush on the test surface after the application of a black background paint. TLC were previously calibrated following the steady-state gradient method [18]. The calibration setup is made by a 4.5 mm thick aluminium rectangular plate, which houses seven thermocouples and is sprayed with black background paint and then TLC. One of its edges is heated by an electric heater, while the other is cooled by air. The whole apparatus is housed into an insulating basis. Camcorder and illuminating system are placed at the same distance and inclination of the real test, so as to replicate the exactly alike optic conditions. A linear temperature gradient will appear on TLC surface: once steady conditions are reached, a single picture is sufficient for a precise measurement of color-temperature response, with the latter parameter measured through thermocouples. Several tests have been carried out, so as to increase global precision; moreover, the calibration has been checked directly on the test article before each experiment.

A digital camera (Sony XCD-SX90CR) records color bitmap images (1280 × 960 pixel) from the TLC painted surface on a PC. The illuminating system (Shott-Fostec KL1500 LCD) uses an optical fiber goose-neck to ensure a uniform illumination on the test surface and it allows to keep both color temperature and light power constant. The test article is completely made of transparent PMMA to allow the required optical access for TLC measurements; the effusion plate only was made of PVC.

2.1. Geometry of the Test Sample. Figure 2 reports a sketch of the test article, which represents the cooling system of the combustor prototype developed within the European Integrated Project NEWAC. A picture of the prototype is shown in Figure 3. The slot coolant representing the starter film cooling is injected in the mainstream from a 6.0 mm high channel, with a lip thickness of 3.0 mm. The effusion array and the dilution hole are fed by an annulus with a rectangular 30.0 mm high and 120.0 mm wide cross-section.

The effusion geometry consists of a staggered array of 272 circular holes ($d = 1.65$ mm), with an inclination angle of $\alpha = 30°$, drilled in a 4.5 mm thick PVC plate and with a length to diameter ratio of $L/D = 5.5$. The spanwise and the streamwise pitches are, respectively, $S_y = 9.9$ mm and $S_x = 12.6$ mm. The first row is located 22.25 mm ($1.77 S_x$) after the slot injection, while the last row 375 mm downstream. The origin of the coordinate system ($x = 0$) was set in order to have $x/S_x = 1$ at the first row and $x/S_x = 29$ at the last row, while the slot injection is located at $x/S_x = -0.77$. The dilution hole ($D = 18.75$ mm) is located immediately after the 14th row, at $x/S_x = 14.16$.

3. Measurement and Test Conditions

The experimental survey was formed by two main campaigns: the first campaign was aimed at measuring the heat transfer
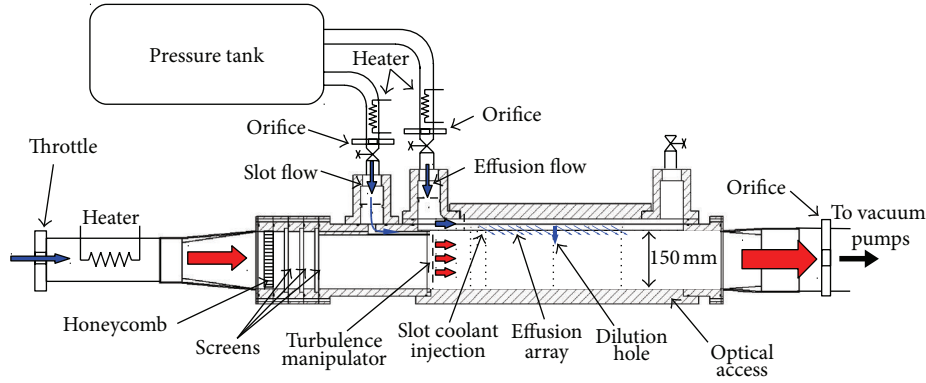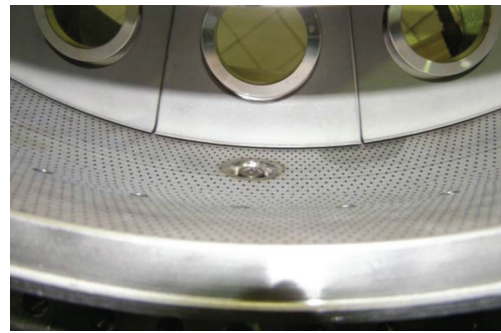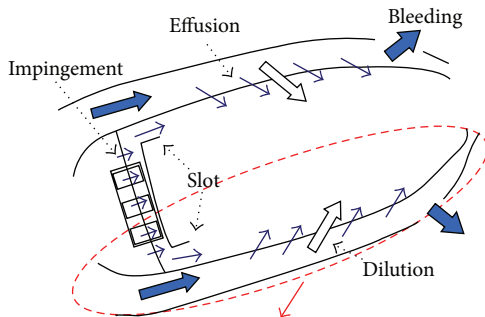
FIGURE 1: Sketch of the test rig.

FIGURE 2: Liner geometry.

FIGURE 3: Combustor prototype of European Project NEWAC.

to estimate the adiabatic effectiveness of the film cooling generated by the system. Results of the two campaigns were finally combined to calculate the Net Heat Flux Reduction and the overall effectiveness.

In modern combustor, the temperature differences between the cooling air and the hot gases lead to a coolant-to-mainstream density ratio which usually falls within the range 1.5–3.0. To reproduce the effects of DR in a low temperature lab-scaled facility, two main approaches are adopted in the literature: cool down the cooling flow or use a foreign gas with a molecular weight greater than the air one. In this work, measurements were carried out by feeding the cooling system with carbon dioxide (CO_2): including the typical temperature differences required to perform experiments with TLC paints, the use of this foreign gas leads to a DR $\approx$ 1.7.

To highlight the effects of density ratio, the test matrix was duplicated and each fluid dynamic condition of the campaign was tested twice: the cooling system was first fed with air and then with CO_2, while air was used for the mainflow. Main investigation parameters are defined as follows:

$$BR_{eff} = \frac{1}{N_{row}} \cdot \sum_{k=1}^{N_{row}} BR_k, \qquad (1)$$
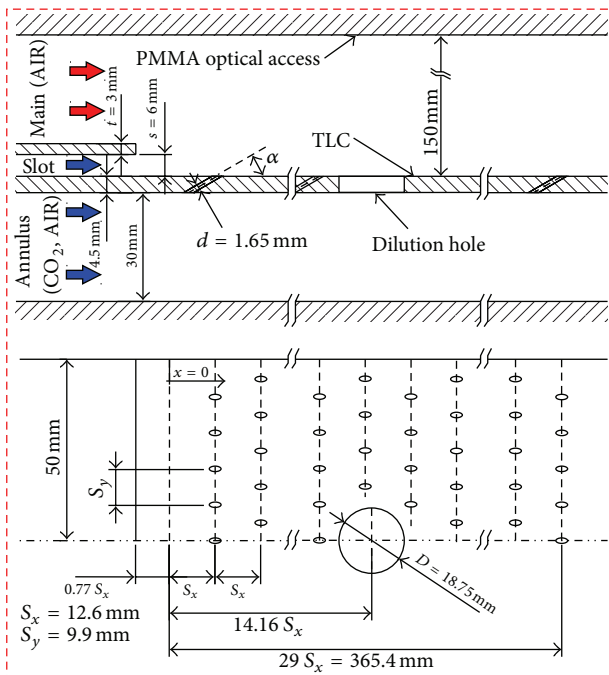
coefficient over the effusion plate, which was tested by imposing values of blowing ratio and velocity ratio within a typical range of an aeroengine combustor. Afterwards the same fluid conditions were replicated in the second campaign in order

$$BR_k = \frac{Cd_k \cdot \left(4 \cdot m_{is,k} / \left(\pi d^2\right)\right)}{m_{main,k}/A_{main}}, \tag{2}$$

$$VR_{eff} = BR_{eff} \cdot \frac{\rho_{main}}{\rho_{cool}} = \frac{BR_{eff}}{DR}. \tag{3}$$

BR_{eff} is the averaged blowing ratio of the effusion rows (the dilution hole was excluded). BR of the kth row was evaluated by using the actual mass flow rate through the holes and the correspondent mainstream mass flow (inlet mainstream mass flow and coolant mass flow injected by the previous $(k-1)$th rows); the amount of coolant crossing each effusion row was calculated by using hole discharge coefficient, which is

$$
\begin{aligned}
Cd &= \frac{m_{real}}{m_{is}} \\
&= \left(m_{real}\right) \times \left(p_{Tc} \left(\frac{p_{main}}{p_{Tc}}\right)^{(\gamma+1)/2\gamma} \right. \\
&\quad \left. \times \sqrt{\frac{2\gamma}{(\gamma-1)\,RT_{Tc}} \left(\left(\frac{p_{Tc}}{p_{main}}\right)^{(\gamma-1)/\gamma} -1\right)\frac{\pi}{4}d^2} \right)^{-1}.
\end{aligned}
\tag{4}
$$

Starting from the cooling and main mass flow and the several pressure values measured along the annulus and in main channel, the procedure uses the previous equations to evaluate the average effusion Blowing Ratio (BR_{eff}). The isentropic mass flow rate of coolant, calculated row by row, and the measured mass flow were employed to estimate a mean value of the effusion discharge coefficient, which is then used to calculate the actual mass flow through each row and consequently the blowing ratio (2). It was estimated that $Cd \approx 0.73$, almost constant for all the tested conditions. Other parameters are

$$
\begin{aligned}
BR_{sl} &= \frac{m_{sl}/A_{sl}}{m_{main}/A_{main}}, \\
BR_{dil} &= \frac{Cd_{dil} \cdot \left(m_{is,dil}/\pi D^2/4\right)}{m_{main,14}/A_{main}}.
\end{aligned}
\tag{5}
$$

A_{main} is the mainstream channel cross-section ($150 \times 100\,mm^2$), A_{sl} is the slot cross-section ($6 \times 100\,mm^2$), and Cd_{dil} was imposed equal to 0.6 [19]. When air is used both as cooling and mainstream flows, the temperature differences of the experiments cannot raise the density ratio over $DR \approx 1.1$ and, as a consequence, tests carried out by imposing the desired values of VR coincide with tests with the correspondent values of BR imposed.

For a better comprehension of slot and effusion influence on the cooling performance, some tests were performed activating only the effusion cooling flow; when the two cooling systems were tested together, the slot flow was set in order to keep a constant value of $BR_{sl} \approx 1.5$. Mainstream absolute pressure was kept constant at about $p_{main} = 50000\,Pa$ ($Re_{main} \approx 75000$, $Ma_{main} \approx 0.04$–0.05), while coolant

TABLE 1: Test matrix.

Flow type (coolant/mainstream)	BR_{eff} (VR_{eff})	VR_{eff} (BR_{eff})
	1.5 (1.5)	—
AIR/AIR	3.0 (3.0)	—
	5.0 (5.0)	—
	7.0 (7.0)	—
	1.5 (0.9)	1.5 (2.6)
CO_2/AIR	3.0 (1.8)	3.0 (5.1)
	5.0 (2.9)	5.0 (8.5)
	7.0 (4.1)	7 (11.9)

pressure was varied to ensure the desired values of coolant velocity inside the holes.

Table 1 sums up the test matrix of the campaign. The effusion plate was first tested using air as coolant, and then using CO_2; 4 different BR_{eff} and 4 different VR_{eff} were investigated. The full test matrix was made up of 48 experiments: each point of Table 1 was tested twice, feeding or not feeding the slot cooling system (8 AIR/AIR and 16 AIR/CO_2 experiments). The resulting 24 experiments matrix was finally performed twice in order to measure HTC and adiabatic effectiveness. It is important to underline that, in reference to the classification introduced by L'Ecuyer and Soechting [20], the effusion jets work within the penetration regime ($VR_{eff} > 0.8$) in all testing conditions.

All the tests were run after steady conditions were reached by all the measured quantities: flow rates, pressures, and temperatures. The uncertainty analysis was performed following the standard ANSI/ASME PTC 19.1 [21] based on the Kline and McClintock method [22]. Temperature accuracy is $\pm0.5\,K$, differential pressure $\pm6.9\,Pa$, and mass flow rate ±3–5%; the estimated error for the heat transfer coefficient calculation is $\pm10\%$, while it is ±0.05 for the adiabatic effectiveness.

4. Data Post Process

4.1. Heat Transfer Measurements. Heat transfer coefficients were determined by a steady-state technique, using TLC paint to measure the wall temperature from a heated surface. The heating element was a $25.4\,\mu m$ thick Inconel Alloy 600 foil; it was laser drilled with the same array pitches of the PVC plate, and then applied on the test plate with a double sided tape. Surface heat flux was generated by Joule effect, fed by a DC power supply (Agilent N5763A) which is connected to the Inconel sheet through two copper bus bars fixed on lateral extremities of the test plate.

The mainstream heat transfer coefficient is defined as

$$HTC_{main} = \frac{q_{conv}}{T_w - T_{main}}, \tag{6}$$

where T_{main} is the mainstream static temperature, measured by means of three thermocouple located one pitch upstream the slot injection. T_w is the wall temperature measured by means of TLC while q_{conv} represents the heat rate exchanged

by convection between the effusion plate and the mainstream flow. Due to the presence of the effusion and dilution holes, heat generated by the Inconel foil is not uniform on the surface of the plate; in addiction, despite the low thermal conductivity of the PVC, test sample is not ideally adiabatic and heat losses due to the conduction through the plate and the convective heat removed by coolant both in the annulus and inside the holes have to be taken into account. As a consequence, in order to have an accurate evaluation of the net heat flux transferred from the surface to the mainstream, q_{conv} was estimated implementing an iterative procedure based on a complete 3D thermal-electric FEM simulation. The procedure evaluates the nonuniform heat locally generated on the surface, allowing to obtain an accurate estimate of q_{conv}. Moreover, heat losses are taken into account too: depending on the fluid dynamics conditions of the tests, they are approximately 2%–5%. A detailed description of the iterative procedure can be found in Facchini et al. [10].

Heat transfer experiments were carried out with coolant and mainstream at room temperature. Likewise effectiveness measurements, the mainstream absolute pressure was kept constant at about $p_{\mathrm{main}} = 50000$ Pa, while coolant pressure was varied in order to ensure the desired values of $\mathrm{BR}_{\mathrm{eff}}$ and $\mathrm{VR}_{\mathrm{eff}}$.

According to Jones [23], the use of a foreign gas requires a special correction during the postprocess of the experimental data (both for heat transfer and effectiveness measurements); this correction allows to take into account the difference in specific heat and thermal conductivity between the foreign gas (CO_2 in this campaign) and the actual cooling flow of a real application (air). Jones assesses that a little correction is necessary in the case of CO_2 injection; in particular, the correction becomes smaller with increasing the coolant velocity (high BR-VR), due to the fact that the transport of species, momentum, and enthalpy becomes mainly dependent on the turbulent flow field rather than on the concentration gradients and the viscosity. Concerning the results of this campaign, whose tests were performed at high BR-VR, it was estimated that the entity of this correction is almost negligible and falls within the error due to the experimental uncertainties.

4.2. Adiabatic Effectiveness Measurements.
Effectiveness measurements were carried out by heating both the coolant and the mainflow, in order to obtain temperature of about 300 K and 350 K, respectively. Likewise HTC measurements, the mainstream absolute pressure was kept constant at about $p_{\mathrm{main}} = 50000$ Pa, while coolant pressure was varied in order to ensure the desired values of coolant velocity.

Adiabatic effectiveness is defined as

$$\eta_{\mathrm{aw}} = \frac{T_{\mathrm{main}} - T_{\mathrm{aw}}}{T_{\mathrm{main}} - T_{\mathrm{cool}}}. \tag{7}$$

Three thermocouples located one pitch upstream the slot injection acquired mainstream static temperature T_{main}. Three additional probes were dedicated to measure coolant flow static temperature and were inserted into the annulus, at $x/S_x = 0; 14; 29$; one further probe was located inside

the slot channel at $x/S_x = -1$. T_{aw} was evaluated through a post-processing procedure which takes into account the thermal fluxes across the plate due to conduction and due to the coolant inside the annulus and the holes. This procedure is based on an 1D approach and considers the following equation:

$$T_{\mathrm{aw}} = T_w - \frac{q}{\mathrm{HTC}_{\mathrm{main}}}, \tag{8}$$

where T_w is the wall temperature measured with TLC. Heat flux across the plate (q) is evaluated through TLC wall temperature and coolant temperature and using the Colburn correlation $\mathrm{Nu} = 0.023\mathrm{Re}^{0.8}\mathrm{Pr}^{1/3}$ to estimate heat transfer coefficients inside the holes and on the annulus side of the plate; Reynolds and Nusselt numbers were evaluated with the hole diameter and with the annulus cross-section hydraulic diameter, respectively. Values of $\mathrm{HTC}_{\mathrm{main}}$ were directly taken from results of the dedicated experimental campaign. Conduction through the PVC was taken into account too.

5. Results

5.1. Heat Transfer Coefficient.
Figure 4 shows heat transfer coefficient maps for the experiments carried out by imposing $\mathrm{BR}_{\mathrm{eff}} - \mathrm{VR}_{\mathrm{eff}} = 3$ (due to the small coolant to mainstream density ratio, $\mathrm{VR}_{\mathrm{eff}} \approx \mathrm{BR}_{\mathrm{eff}}$ in AIR tests); results are displayed dividing the local $\mathrm{HTC}_{\mathrm{main}}$ by a constant reference value ($\mathrm{HTC}_{\mathrm{ref}}$). In white areas close to the dilution hole HTC was not measured because the local low/high surface heat generation did not allow TLC paints working properly within their activation range. Maps displays the overall trend of HTC, showing that it increases up to the 14th row and then remains nearly constant. Difference between tests with and without slot is restricted to the first 2-3 rows, where coolant coming out from the slot mitigates the heat transfer; after the 5th row, the presence of the slot flow does not alter significantly the behaviour of the effusion cooling.

Imposing the same mainstream conditions of all the other experiments, a reference test was carried out in order to evaluate the heat transfer coefficient without film cooling (HTC_0); map of HTC_0 is displayed in Figure 4. Values of HTC_0 were spanwise averaged and the resulting trend along the centerline was used as the reference.

Figures 5(a) and 5(b) show trends of spanwise averaged heat transfer coefficient along the plate with effusion coolant only and with both slot and effusion flows for $\mathrm{BR}_{\mathrm{eff}} - \mathrm{VR}_{\mathrm{eff}} = 3$; data are plotted in terms of ($\mathrm{HTC}_{\mathrm{main}}/\mathrm{HTC}_0$) in order to highlight the increase of heat transfer due to coolant injections. Figure 5(a) shows that HTC remains constant in the first five rows, even if it is enhanced compared to the reference case ($\mathrm{HTC}_{\mathrm{main}}/\mathrm{HTC}_0 > 1$); after the 5th row, it increases up to the dilution hole, where it reaches an asymptotic value. The beginning of the rising trend of HTC is brought forward to the 2-3th row in presence of the slot cooling flow (Figure 5(b)); however, as it was already shown in the maps, after the 5th row, the slot flow has only a slight influence on the heat transfer. Results show
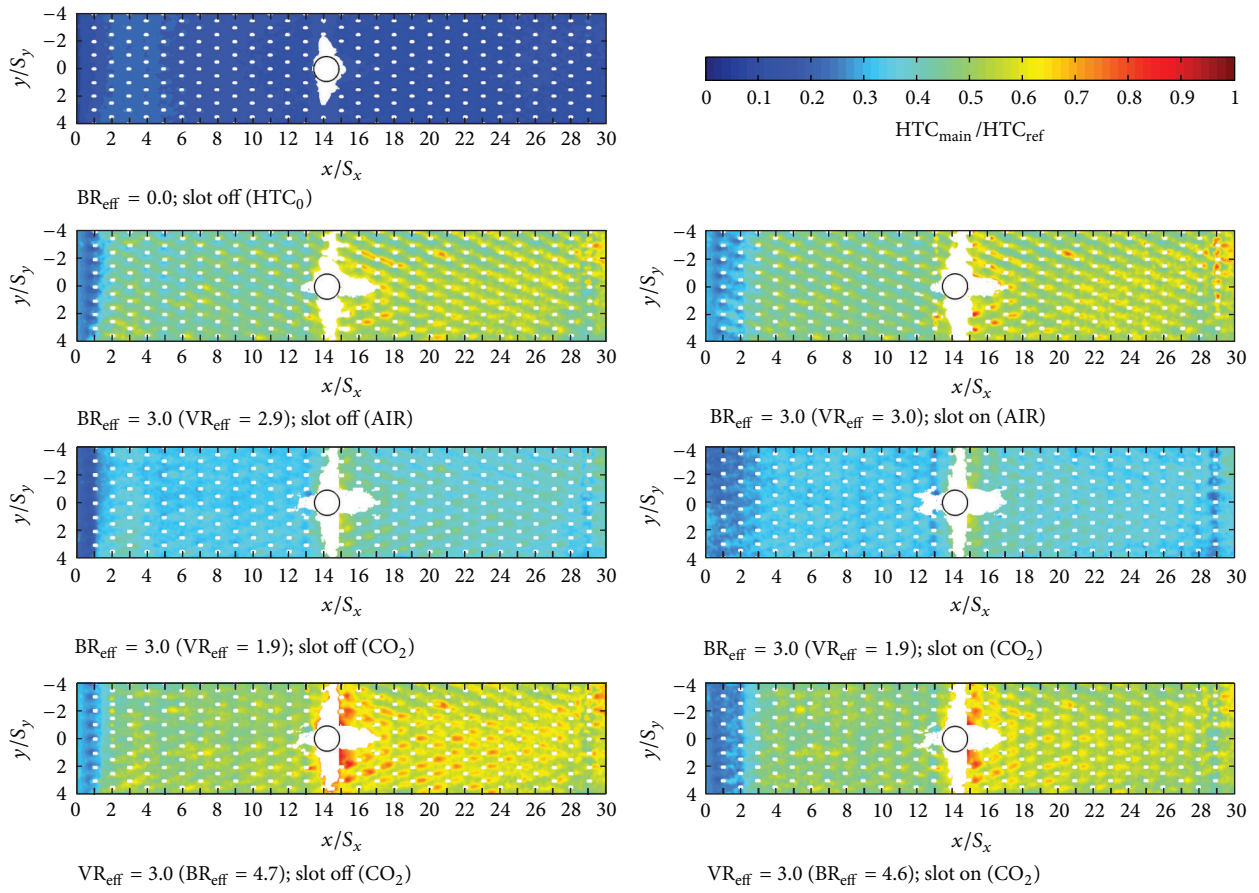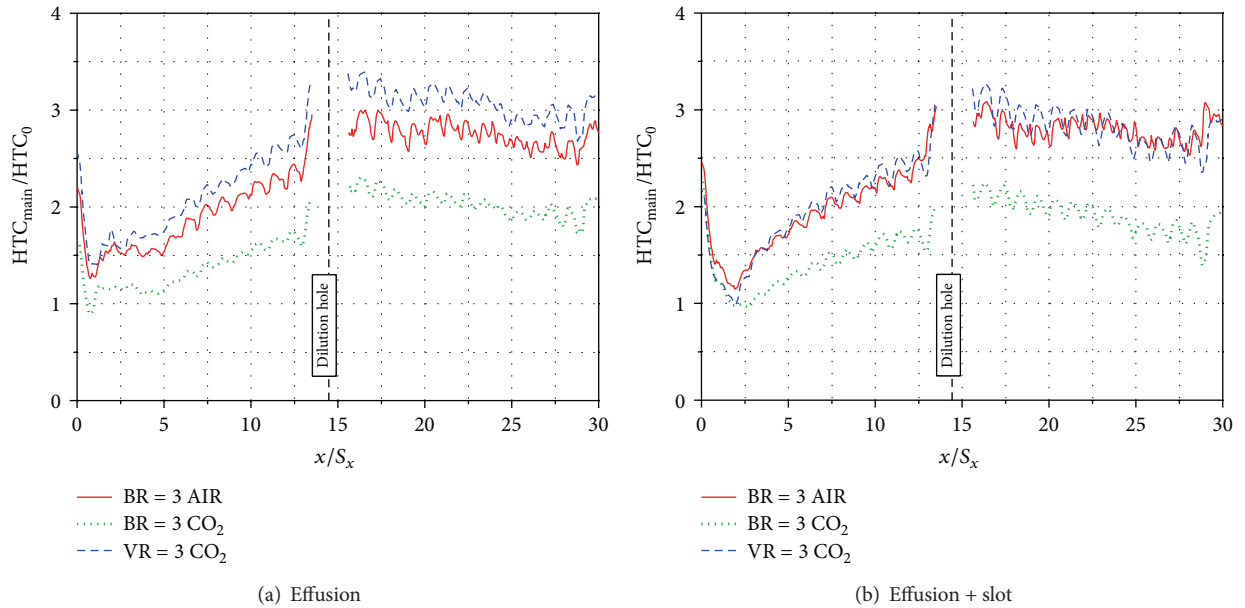
FIGURE 4: Heat transfer coefficients maps ($BR_{eff} - VR_{eff} = 3$).

(a) Effusion

(b) Effusion + slot

FIGURE 5: Spanwise averaged HTC ($BR_{eff} - VR_{eff} = 3$).

(a) Averaged value of HTC/HTC_0 versus BR_{eff}

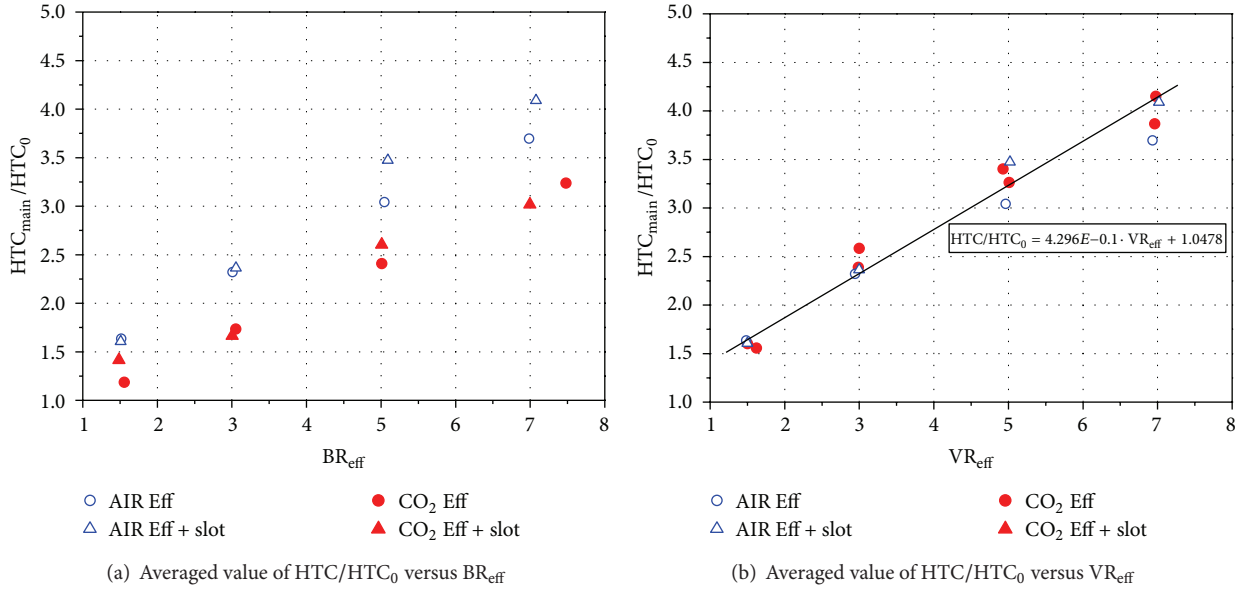(b) Averaged value of HTC/HTC_0 versus VR_{eff}

FIGURE 6: Heat transfer coefficient results.

that for a constant blowing ratio, heat transfer decreases with increasing density ratio; on the other hand, results of tests carried out by imposing the same value of velocity ratio are almost coincident. Maps and trends are here shown only for one point of the test matrix, which significantly represents the typical behaviour of the system in each testing condition. A more detailed description of the behaviour of heat transfer coefficient over this effusion plate can be found in Facchini et al. [10]. Results of the full test matrix are summarized in Figure 6: it shows the average value of HTC_{main}/HTC_0 of the whole plate with and without the slot flow, plotted versus the actual BR_{eff} Figure 6(a) and VR_{eff} Figure 6(b). Figures clearly display how the HTC linearly increases with increasing BR-VR; furthermore, it is possible to highlight that air tests are in good agreement with CO_2 tests with the same velocity ratio (Figure 6(b)). This means that, within the effusion jets penetration regime, VR acts as the driving parameter of the phenomena instead of BR; this confirms the results numerically found by Andreini et al. [16]. Figure 6(b) includes also the equation of the linear fitting of the experimental data: the maximum estimated relative error was around 10%, while the averaged value was around 4.5%. Even if the outcomes of the campaign are affected by a low turbulence level with respect to an actual combustor, results give useful information about the behaviour of the effusion system and, moreover, show that the use of velocity ratio in a low temperature facility allows reproduction of the effects of DR without employing a foreign gas.

5.2. Adiabatic Effectiveness.

Figure 7 shows the adiabatic effectiveness maps for $BR_{eff} - VR_{eff} = 3$ test points. Maps display the effects of effusion and slot coolant injections and highlight both how the wake generated by the dilution hole and the presence of the slot flow influence the film cooling distribution over the surface. Results point out that,

without the slot flow, the effusion system does not guarantee a sufficient protection of the first part of the liner by itself. On the other hand, maps with both effusion and slot coolant show that a very efficient protection of the liner can be obtained combining the two cooling systems.

Figure 8 shows trends of spanwise averaged adiabatic effectiveness along the plate: it is possible to observe that, when only effusion is activated, the film cooling superposition increases η_{aw} quite linearly until the 15th row, where the dilution hole is located. In the following rows, the wake generated by the dilution hole deeply affects the film distribution: a slight decrease of effectiveness can be observed immediately downstream the hole, after which the dilution jet draws the coolant from the effusion holes towards the center of the test palate and generates a high effectiveness area. The effective level in this area is almost asymptotic until the end of the plate.

Focusing on the effects of DR on test, it is possible to observe that an increase of VR_{eff} leads to a slight increase in η_{aw}; moreover, even if the differences among the curves are quite small, BR_{eff} seems to be the parameter which allows to take into account the effects of density ratio even in air-to-air tests.

The presence of the slot coolant strongly enhances the adiabatic effectiveness; after the first three rows where the η_{aw} remains nearly constant, there is a lower effectiveness area due to the detrimental interaction between the two cooling flows: here the highly penetrating effusion jets partially destroy the high effectiveness film cooling layer generated by the slot [9]. This behaviour can be directly related to the velocity ratio of the jets, which can be used to scale the effects of DR; after the dilution hole, η_{aw} reaches an asymptotic value which can still be related to the velocity ratio.

Finally Figure 9 shows the adiabatic effectiveness results for the whole test matrix, plotted versus BR_{eff} and VR_{eff}; each point represents the averaged value of the entire test sample.
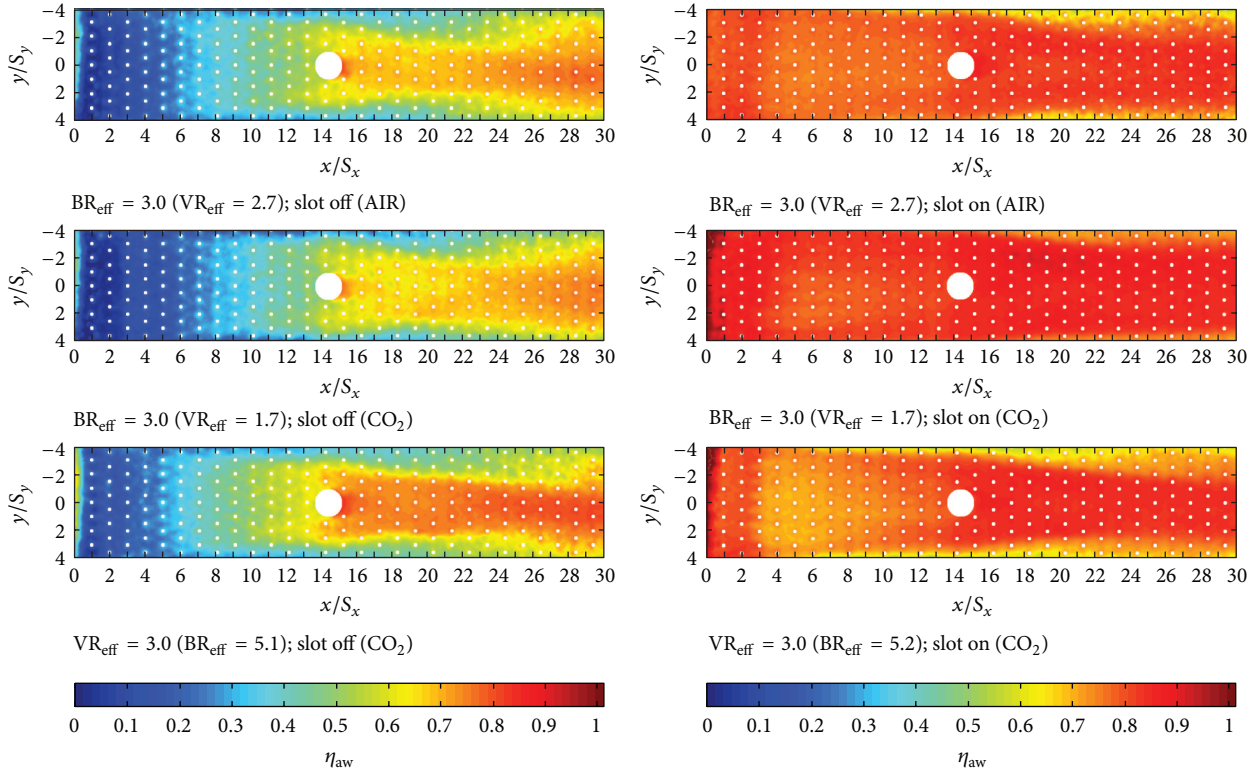
Figure 7: Adiabatic effectiveness maps ($BR_{eff} - VR_{eff} = 3$).
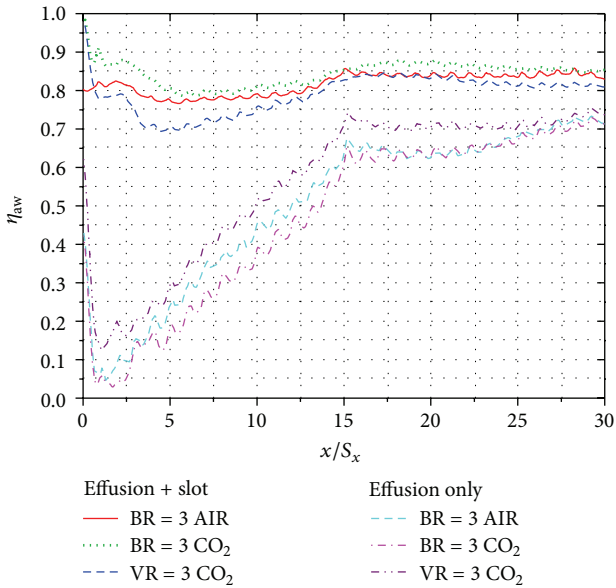
Figure 8: Spanwise averaged η_{aw} ($BR_{eff} - VR_{eff} = 3$).

Tests without slot flow (circles) confirm the outcomes from the analysis of Figure 8: experimental results show that within the penetration regime, the effects of coolant to mainstream density ratio are small thus, as commonly found in the literature, BR have to be used to scale the effects of DR.

In addition, results allow the highlight of the behaviour of the system at high values of BR-VR: here η_{aw} is only weakly affected by those parameters since the high effectiveness is mainly due to the coolant mass addiction. In fact, even if the penetration of effusion jets increases, η_{aw} does not fall because the large amount of coolant mass flow injected in the mainstream grows row by row and guarantees the good protection of the liner.

Concerning tests with both cooling systems (triangles), results indicate that η_{aw} decreases with increasing BR-VR (due to the increasing penetration of effusion jets), but only slight differences were found changing the coolant to mainstream density ratio. Focusing on tests with the same BR_{eff} Figure 9(a), it is possible to note that an increase in DR causes a small enhancement in η_{aw}; on the other hand, results indicate that when both the slot flow and the effusion are active and the jets work within the penetration regime, VR_{eff} has to be used to take into account the effects of density ratio.

5.3. Net Heat Flux Reduction and Overall Effectiveness. Net Heat Flux Reduction (NHFR) is a commonly used parameter to evaluate the reduction of heat flux across a cooled surface. This parameter was defined by Sen et al. [24] as

$$NHFR = 1 - \frac{q}{q_0} = 1 - \frac{HTC_{main}}{HTC_0}\left(1 - \eta\theta\right), \qquad (9)$$

(a) Averaged value of η_{aw} versus BR_{eff}

○ AIR Eff	● CO_2 Eff
△ AIR Eff + slot	▲ CO_2 Eff + slot

(b) Averaged value of η_{aw} versus VR_{eff}

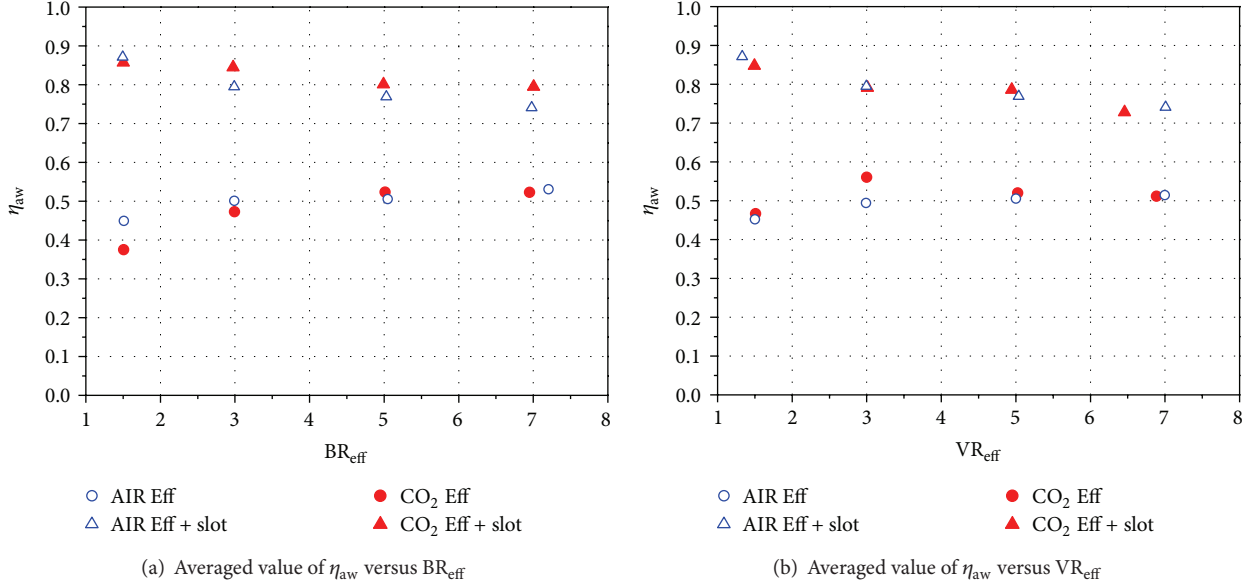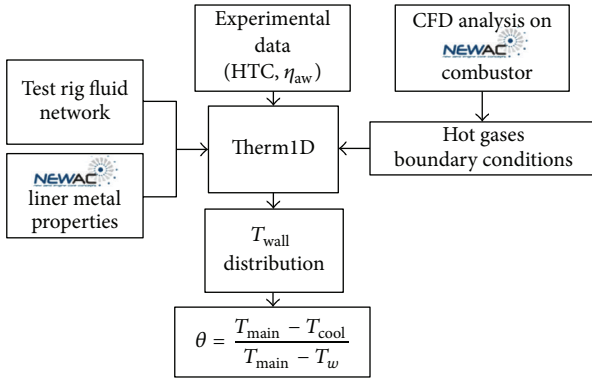| ○ AIR Eff	● CO_2 Eff
△ AIR Eff + slot	▲ CO_2 Eff + slot

FIGURE 9: Adiabatic effectiveness results.

FIGURE 10: Procedure to evaluate θ.

where θ represent the dimensionless temperature:

$$\theta = \frac{T_{main} - T_{cool}}{T_{main} - T_w}. \qquad (10)$$

In the open literature [24–27], NHFR was mainly used to evaluate turbine endwall and blades cooling systems and the dimensionless temperature was set within the range of $\theta = 1.5$–1.6. Since the overall effectiveness of a combustor cooling system is generally higher than the one of a turbine airfoil, more recently Facchini et al. [10, 11] updated this parameter to evaluate the NHFR of a cooled liner, imposing a value of $\theta = 1.2$. In the present study, NHFR was evaluated by using the experimental results within a one-dimensional thermal procedure (Therm1d) in order to estimate an engine representative distribution of θ. Therm1d is an in-house procedure which solves heat conduction inside a combustor liner and provides its temperature distribution by using

an 1D Finite Difference Model. On the coolant side, the procedure solves the coolant fluid network of the system, taking into account the different cooling techniques of the specific combustor architecture and the heat exchange with metal surfaces; on the hot gas side, it estimates the convective heat load and the luminous and the nonluminous radiation through a correlative approach, mainly following the one-dimensional approach suggested by Lefebvre [19]. The final temperature distribution is obtained considering also the film cooling, usually estimated through correlations, and the heat sink effect due to the presence of cooling holes. Further details on the procedure can be found in Andreini et al. [28, 29].

Figure 10 illustrates the procedure followed to estimate the NHFR of the cooling scheme in engine representative working conditions. Therm1d was used to set up the cooling fluid network of the test rig, including both the slot and the effusion system; test plate material was specified to be the real steel of NEWAC combustor prototype instead of PVC as in the experiments to more realistically model the conduction through the plate itself. Moreover, hot gas boundary conditions (i.e., gas temperature, pressure, etc.), taken from previous CFD analysis on the NEWAC combustor, were imposed in order to simulate the behaviour of a realistic combustor diffusion flame and, consequently, to estimate realistic the heat loads [28]. As an example, Figure 11(a) shows the distribution of mainstream gas temperature inside the core of the combustor (temperatures are adimensionalized with a reference value): it is possible to identify the position of the flame front, which causes the temperature rise downstream the second row. Coolant side inlet pressure was varied in order to set the desired averaged BR-VR through the effusion holes and reproduce the experimental test matrix, while inlet coolant temperature and outlet pressure were kept
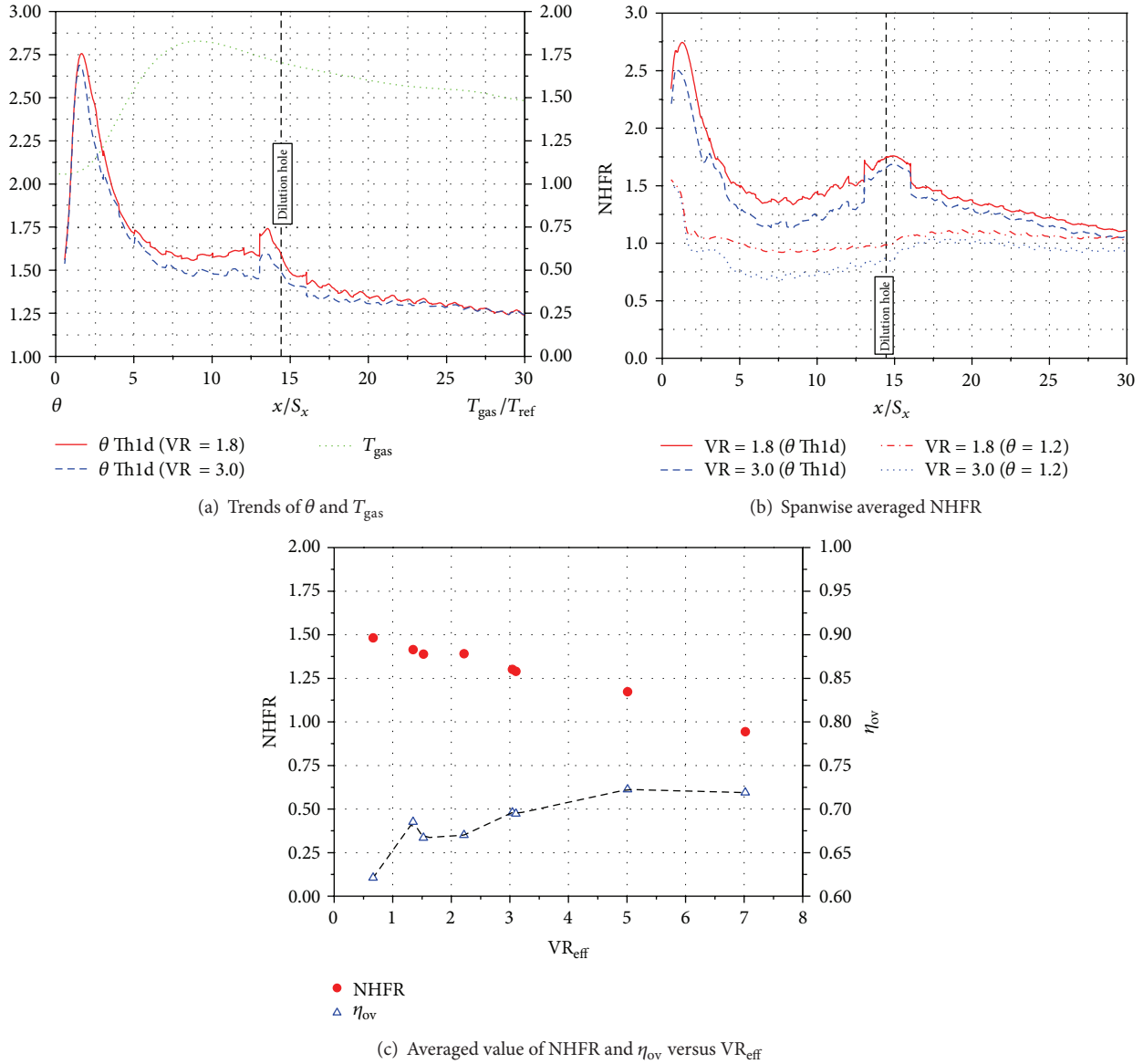
(a) Trends of θ and T_{gas}

θ Th1d (VR = 1.8) ⋯⋯ T_{gas}
θ Th1d (VR = 3.0)

(b) Spanwise averaged NHFR

—— VR = 1.8 (θ Th1d) ·—·— VR = 1.8 (θ = 1.2)
— — VR = 3.0 (θ Th1d) ⋯⋯ VR = 3.0 (θ = 1.2)

● NHFR
△ η_{ov}

(c) Averaged value of NHFR and η_{ov} versus VR_{eff}

FIGURE 11: Net Heat Flux Reduction and η_{ov} results.

constant. Experimental film cooling and convective gas side HTC distributions obtained in this work were imposed as boundary conditions too: in order to take into account the effects of density ratio due to the temperature difference between coolant and mainstream, data were taken only from CO_2 tests (only tests with both effusion and slot cooling system). This procedure allowed simulation of the behaviour of the cooling system under realistic operating condition and to finally estimate the distribution of NHFR along the liner: in fact, each run provided the liner surface temperature distributions (T_w) and the local temperature of the coolant coming out from each effusion row (T_{cool}), including its heating through the hole due to the heat removal by heat sink effect.

Figure 11(a) shows trends of the θ parameter for cases $BR_{\text{eff}} = 3\,(VR_{\text{eff}} \simeq 1.8)$ and $VR_{\text{eff}} = 3$. It is possible to observe how θ varies along the liner as a consequence of a nonuniform mainstream temperature distribution and of the resulting T_{cool} and T_w; it can be noticed that an increase in VR_{eff} leads to a slight decrease of θ.

Figure 11(b) displays trends of NHFR for the two previous test points: results evaluated through *Therm1d* are compared with those estimated by imposing a constant value of $\theta = 1.2$. As a consequence of the θ behaviour, NHFR calculated considering the heat sink effect is much higher than the simple θ-imposed case (the averaged value is almost 30% higher). Obviously trends evaluated with *Therm1d* are highly affected by the hot gases imposed boundary conditions (e.g., the drop

after the 2th row is related to the gas temperature rise which represents the flame front), but what is important to highlight is the influence of effusion velocity ratio on NHFR. Even if NHFR linearly decreases with VR_{eff}, Figure 11(c) points out that the cooling system always brings to a reduction of the heating flux towards the liner (NHFR > 0).

Despite previous considerations, NHFR is not properly representative for an effusion cooling system since its definition (9) does not explicitly take into account the heat sink effect, which instead plays a major role in this type of cooling technique. To overcome this aspect and give a complete description of the cooling performance of the system, wall temperatures estimated through *Therm1d* were finally employed to calculate also the overall effectiveness of the test plate in real engine conditions. This further parameter indicates the overall cooling capability of a cooling system and is defined as:

$$\eta_{ov} = \frac{T_{main} - T_w}{T_{main} - T_{cool}}. \tag{11}$$

Results depicted in Figure 11(c) show that, except for very low values of velocity ratio, η_{ov} remains high and almost constant for a wide range of operative conditions; even if results do not take into account the effects of turbulence, whose level is rather lower than a real combustor, they give useful indications for the designer: in fact, this study points out that the combined effusion and slot system is very effective and robust from a cooling point of view for a wide range of operative conditions. As a consequence, this flexibility of the system allows, during the design phase, to focus its optimization taking into account other requirements, like combustion issues, aeroacoustic or simply off-design working conditions.

6. Conclusions

The aim of the present study is the investigation of the effects of coolant-to-mainstream density ratio on the cooling performance of a real engine cooling scheme of a combustor liner. The cooling scheme consists of a slot injection, followed by a flat plate with 29 effusion rows and a single large dilution hole. Values of effusion blowing ratio and velocity ratio typical of modern engine working conditions were imposed in order to measure the heat transfer coefficient and the adiabatic effectiveness; tests were carried out by using a steady-state technique with wide band thermochromic liquid crystals. To obtain a value of density ratio which is representative for a combustor, tests were carried out by feeding the cooling system with a foreign gas (CO_2).

HTC results show that, for a constant blowing ratio, heat transfer is reduced with increasing the density ratio; on the other hand, within the effusion jets penetration regime, velocity ratio is the driving parameter of the phenomena in order to scale the effects of DR. Concerning the adiabatic effectiveness, experiments show that after $VR_{eff} = 3$, η_{aw} generated by the effusion jets is weakly affected by BR-VR; furthermore, effects of density ratio can be neglected within the penetration regime. When both slot and effusion system are activated, results point out that, for a constant velocity ratio, effectiveness increases with increasing density ratio and that VR_{eff} can be used to take into account the effects of DR.

Finally, NHFR and the overall effectiveness were estimated combining heat transfer and effectiveness results: real engine working conditions were simulated by using an in-house 1D thermal procedure. Results point out a linear decrease of NHFR with VR_{eff}, even if the system always brings a reduction of the heating flux towards the liner; results in terms of η_{ov} indicate that the combined effusion and slot cooling system has a very effective and robust behaviour over a wide range of operative conditions.

Nomenclature

A: Reference area (m^2)
BR: Blowing ratio (−)
Cd: Hole discharge coefficient (−)
d: Effusion hole diameter (m)
D: Dilution hole diameter (m)
DR: Density ratio (−)
HTC: Heat transfer coefficient (W/m^{2}K)
L: Hole length (m)
Ma: Mach number (−)
m: Mass flow rate (kg/s)
p: Pressure (Pa)
q: Heat flux (W/m^2)
Re: Reynolds number (−)
s: Slot lip thickness (m)
S_x: Streamwise pitch (m)
S_y: Spanwise pitch (m)
T: Temperature (K)
VR: Velocity ratio (−)
x: Abscissa along the plate (m)
y: Spanwise location (m).

Greeks

α: Effusion hole injection angle (deg)
η: Effectiveness (−)
γ: Ratio of specific heat (−)
θ: Dimensionless temperature (−)
ρ: Density (kg/m^3).

Subscript

aw: Adiabatic wall
c: Coolant
conv: Convection
eff: Effusion
is: Isentropic
main: Mainstream
ov: Overall
ref, 0: Reference
sl: Slot
T: Total
w: Wall.

Acronyms

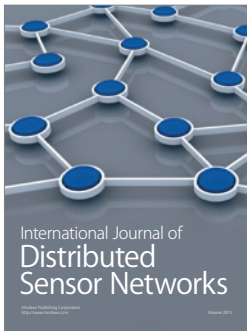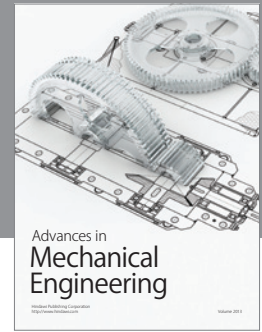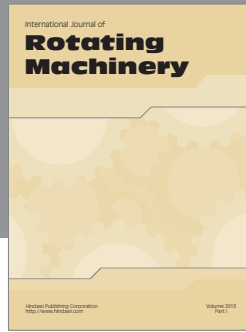|	
CO_2:	Carbon dioxdide
FEM:	Finite Element Method
ICAO:	International Civil Aviation Organization
NEWAC:	NEW Aeroengine Core concept
NHFR:	Net Heat Flux Reduction
OTDF:	Outlet Temperature Distribution Factor
PMMA:	Poly(methyl methacrylate)
PVC:	Polyvinyl chloride
TLC:	Thermochromic Liquid Crystal.

Acknowledgments

References

[1] G. E. Andrews, F. Bazdidi-Tehrani, C. I. Hussain, and J. P. Pearson, "Small diameter film cooling hole heat transfer: the influence of hole length," ASME Paper 91-GT-344, 1991.

[2] G. E. Andrews, I. M. Khalifa, A. A. Asere, and F. Bazdidi-Tehrani, "Full coverage effusion film cooling with inclined holes," ASME Paper 95-GT-274, 1995.

[3] J. J. Scrittore, K. A. Thole, and S. W. Burd, "Experimental characterization of film-cooling effectiveness near combustor dilution holes," ASME Turbo Expo GT2005-68704, 2005.

[4] J. J. Scrittore, K. A. Thole, and S. W. Burd, "Investigation of velocity profiles for effusion cooling of a combustor liner," ASME Turbo Expo GT2006-90532, 2006.

[5] D. E. Metzger, D. I. Takeuchi, and P. A. Kuenstler, "Effectiveness and heat transfer with full-coverage film cooling," *ASME Journal of Engineering For Power*, vol. 95, no. 3, pp. 180–184, 1973.

[6] M. E. Crawford, W. M. Kays, and R. J. Moffat, "Full-coverage film cooling-2. Heat transfer data and numerical simulation," *Journal of engineering for power*, vol. 102, no. 4, pp. 1006–1012, 1980.

[7] R. F. Martinez-Botas and C. H. N. Yuen, "Measurement of local heat transfer coefficient and film cooling effectiveness through discrete holes," ASME Turbo Expo 2000-GT-243, 2000.

[8] G. B. Kelly and D. G. Bogard, "An investigation of the heat transfer for full coverage film cooling," ASME Turbo Expo GT2003-38716, 2003.

[9] A. Ceccherini, B. Facchini, L. Tarchi, and L. Toni, "Combined effect of slot injection, effusion array and dilution hole on the cooling performance of a real combustor liner," ASME Turbo Expo GT2009-60047, 2009.

[10] B. Facchini, F. Maiuolo, L. Tarchi, and D. Coutadin, "Combined effect of slot injection, effusion array and dilution hole on the heat transfer coefficient of a real combustor liner-part 1 experimental analysis," ASME Turbo Expo GT2010-22936, 2010.

[11] B. Facchini, F. Maiuolo, L. Tarchi, and D. Coutadin, "Experimental investigation on the effects of a large recirculating area on the performance of an effusion cooled combustor liner," *Journal of Engineering For Gas Turbines and Power*, vol. 134, no. 4, Article ID 041505, 2012.

[12] S. V. Ekkad, D. Zapata, and J. C. Han, "Film effectiveness over a flat surface with air and CO2 injection through compound angle holes using a transient liquid crystal image method," *Journal of Turbomachinery*, vol. 119, no. 3, pp. 587–593, 1997.

[13] S. V. Ekkad, D. Zapata, and J. C. Han, "Heat transfer coefficients over a flat surface with air and CO2 injection through compound angle holes using a transient liquid crystal image method," *Journal of Turbomachinery*, vol. 119, no. 3, pp. 580–586, 1997.

[14] Y. Lin, B. Song, B. Li, G. Liu, and Z. Wu, "Investigation of film cooling effectiveness of full-coverage inclined multihole walls with different hole arrangements," ASME Turbo Expo GT2003-38881, 2003.

[15] Y. Lin, B. Song, B. Li, and G. Liu, "Investigation of film cooling effectiveness of full-coverage inclined multihole walls with different hole arrangements," *ASME Journal of Heat Transfer*, vol. 128, no. 6, pp. 580–585, 2006.

[16] A. Andreini, A. Ceccherini, B. Facchini, and D. Coutadin, "Combined effect of slot injection, effusion array and dilution hole on the heat transfer coefficient of a real combustor liner-part 2 numerical analysis," ASME Turbo Expo GT2010-22937, 2010.

[17] P. E. Roach, "The generation of nearly isotropic turbulence by means of grids," *International Journal of Heat and Fluid Flow*, vol. 8, no. 2, pp. 82–92, 1987.

[18] T. L. Chan, S. Ashforth-Frost, and K. Jambunathan, "Calibrating for viewing angle effect during heat transfer measurements on a curved surface," *International Journal of Heat and Mass Transfer*, vol. 44, no. 12, pp. 2209–2223, 2001.

[19] A. H. Lefebvre, *Gas Turbine Combustion*, Taylor & Francis, London, UK, 1998.

[20] M. R. L'Ecuyer and F. O. Soechting, "A model for correlating flat plate film cooling effectiveness for rows of round holes," in *AGARD Heat Transfer and Cooling in Gas Turbines 12p (SEE N86-29823 21-07)*, 1985.

[21] The American Society of Mechanical Engineers, "Measurement uncertainty," in *Instrument and Apparatus, Volume ANSI/ASME PTC 19.1-1985 of Performance Test Code*, The American Society of Mechanical Engineers, New York, NY, USA, 1985.

[22] S. J. Kline and F. A. McClintock, "Describing uncertainties in single sample experiments," *Mechanical Engineering*, vol. 75, pp. 3–8, 1953.

[23] T. V. Jones, "Theory for the use of foreign gas in simulating film cooling," *International Journal of Heat and Fluid Flow*, vol. 20, no. 3, pp. 349–354, 1999.

[24] B. Sen, D. L. Schmidt, and D. G. Bogard, "Film cooling with compound angle holes: heat transfer," *Journal of Turbomachinery*, vol. 118, no. 4, pp. 800–806, 1996.

[25] M. Gritsch, A. Schulz, and S. Wittig, "Film-cooling holes with expanded exits: near-hole heat transfer coefficients," *International Journal of Heat and Fluid Flow*, vol. 21, no. 2, pp. 146–155, 2000.

[26] J. R. Christophel, K. A. Thole, and F. J. Cunha, "Cooling the tip of a turbine blade using pressure side holes-part ii: heat transfer measurements," *ASME Turbo Expo*, no. 2004-GT-53254, 2005.

[27] J. D. Piggush and T. W. Simon, "Measurements of net change in heat flux as a result of leakage and steps on the contoured endwall of a gas turbine first stage nozzle," *Applied Thermal Engineering*, vol. 27, no. 4, pp. 722–730, 2007.

[28] A. Andreini, C. Carcasci, A. Ceccherini et al., "Combustor liner temperature prediction: a preliminary tool development and its application on effusion cooling systems," in *Proceedings of the 1st CEAS European Air and Space Conference Century Perspectives*, Paper n.026, 2007.

[29] A. Andreini, A. Ceccherini, B. Facchini, F. Turrini, and I. Vitale, "Assesment of a set of numerical tools for the design of aeroengines combustors: study of a tubular test rig," ASME Turbo Expo GT2009-59539, 2009.